Articles

$CePS_4$ Electronic Structure and Optical Properties

G. Gauthier,[†] S. Jobic,[†] F. Boucher,[†] P. Macaudière,[‡] D. Huguenin,[‡] J. Rouxel,[†] and R. Brec*[,†,§]

Laboratoire de Chime des Solides, Institut des Matériaux de Nantes, UMR 6502 CNRS-Université de Nantes, 2 rue de la Houssinière, BP 32229, 44322 Nantes Cedex 3, France, and Rhodia Recherches, 52 rue de la Haie Coq, 93308 Aubervilliers, France

Received April 8, 1998. Revised Manuscript Received May 28, 1998

The structure of $CePS_4$ has been determined from single-crystal X-ray diffraction data ($I4_1/acd$ space group, $a = b = 10.9228(3)$ Å, $c = 19.3998(6)$ Å, $V = 2314.5(2)$ Å^3, $Z = 16$). The refinement, conducted from 547 independent reflections ($I > 3\sigma(I)$ and 30 variables) led to R_F (%) = 1.83 and R_{wF} (%) = 2.36. Diffuse reflectance spectra of $CePS_4$ and of the $La_{1-x}Ce_xPS_4$ series indicated that the electronic absorption mechanism in $CePS_4$, a $4f^1 \rightarrow 5d^0$ transition on the Ce^{III} ions, is the same as in γ-Ce_2S_3, with only the band gap width being modified. To this transition corresponds an absorption threshold responsible for the yellow hue of the thiophosphate at about 2.5 eV. Band structure calculation (TB-LMTO-ASA) confirms the experimental evidence of the Ce^{III} $4f^1 \rightarrow 5d^0$ transition. Comparisons between $CePS_4$ and γ-Ce_2S_3 through their electronic localized functions revealed the inductive effect of the P−S covalent bonding on the Ce−S bond, with the resulting increase of the Ce^{III} $4f^1 \rightarrow 5d^0$ transition in the thiophosphate as compared to the sulfide. This increase is ascribed, in part, to a lowering of the 4f block because of the decreased screening effect of the more ionic Ce−S bonding in $CePS_4$.

Introduction

In a previous study on the crystal and electronic structure of sodium-doped cerium sulfide $Na_{3x}Ce_{2-x}S_3$ compounds, [1] it was shown that the red color of these materials was to be attributed to an absorption corresponding to the Ce^{III} atom-like band-based $4f^1 \rightarrow 5d$ electronic transition. The insertion−substitution of alkali-metal (Li, Na, K ...) into the Th_3P_4-type structure of cation deficient γ-Ce_2S_3 ($Ce_{8/3}\square_{1/3}S_4$) resulted in a color change of the pristine material, the phase evolving from red-burgundy to bright-red in the $Na_{3x}Ce_{2-x}S_3$ series ($0 < x < 0.125$), in accord with the overall increased ionicity of the phase.[2] This color change, related to the widening of the $4f^1 \rightarrow 5d^0$ energy gap by about 0.1 eV, was observed from the threshold energies of the diffuse reflection spectra and from powder photocurrent measurements.[3] To study the inductive effect[4−7] on the Ce−S bond and its consequences on this particular electronic transition, we decided to turn toward $CePS_4$ since this phase presents a completly different absorption energy gap as evidenced by its bright-yellow color.[8] We thus embarked on the synthesis of this material to determine its optical properties but, because neither its accurate crystal nor its electronic structure were known, an attempt to synthesize single crystals of the phase was first made. We hence report the successful preparation of $CePS_4$ single crystals and the precise structure determination of the compound, followed by its band structure determination. In addition, numerous compositions of the $La_{1-x}Ce_xPS_4$ solid solution were synthesized to confirm the nature of the optical transition inducing the color of $CePS_4$, through UV−visible diffuse reflection spectra recording. The electronic structure scheme of the compound has been then studied in relation with its optical properties and by comparison with the γ-Ce_2S_3 phase to explain the chromatic differences between the two materials and to unravel the influence of phosphorus on the Ce 4f−5d energy gap.

Experimental Section

Synthesis of $CePS_4$ and of the $La_{1-x}Ce_xPS_4$ Series ($0 \leq x < 1$). $CePS_4$ and the solid solutions of several $La_{1-x}Ce_xPS_4$

[†] Institut des Materiaux de Nantes.
[‡] Rhodia Recherches.
[§] Tel: (33) 2-40-37-39-16. Fax: (33) 2-40-37-39-95. e-mail: brec@cnrs-imn.fr.

(1) Mauricot, R.; Evain, M.; Gressier, P.; Brec, R. *J. Alloys Compd.* **1995**, *223*, 130.
(2) Zhukov, V.; Mauricot, R.; Gressier, P.; Evain, M. *J. Solid State Chem.* **1997**, *128*, 197.
(3) Mauricot, R. Thesis, University of Nantes, France, 1995.
(4) March, J. *Advanced Organic Chemistry*, 3rd ed.; John Wiley: New York, 1985.
(5) Noll, W. *Angew. Chem., Int. Ed. Engl.* **1963**, *2*, 73.
(6) Shannon, R. D. *Chem. Commun.* **1971**, 881.
(7) Etourneau, J.; Portier, J.; Ménil, F. *J. Alloys Compd.* **1992**, *188*, 1.
(8) Huang, Z.; Cajipe, V. B.; Le Rolland, B.; Colombet, P.; Schipper, W. J.; Blasse, G. *Eur. J. Solid State Inorg. Chem.* **1992**, *29*, 1133.

S0897-4756(98)00711-X CCC: $15.00
Published on Web 08/13/1998

Table 1. Crystallographic Data and Experimental Details for $CePS_4$

Physical and Crystallographic Data	
formula: $CePS_4$	molar mass: 299.369
color: yellow	crystal size (mm^3): $0.1 \times 0.1 \times 0.15$
system: tetragonal	space group: $I4_1/acd$ (No. 142)
cell params (powder refinement, $T = 300$ K): $a = b = 10.9228(3)$ Å, $c = 19.3998(6)$ Å, $V = 2314.5(2)$ Å^3, $Z = 16$, $d_{calcd} = 3.435$ g cm^{-3}	
linear abs coeff:	$\mu(\lambda_{MoK-L2,3}) = 94.97$ cm^{-1}
Recording Conditions	
temperature: 293 K	diffractometer: CAD4-F
radiation: $\lambda_{MoK-L2,3} = 0.71069$ Å	
monochromator: oriented graphite (002)	scan mode: ω/θ
angular range 2θ (deg): 3.0−70.0	hkl range: $-5 \le h \le 17$, $-5 \le k \le 17$, $-5 \le l \le 31$
standard reflectns: (4 2 4), (4 −2 4), (−4 −2 −4)	
abs correction: semiempirical based on ψ scans	
transm coeff: 0.0624 − 0.1156	
Data Reduction	
total recd reflectns: 13112	obsd reflectns ($I > 3\sigma(I)$): 2287
independent reflections ($I > 3\sigma(I)$): 547	R_{int} (%) = 3.19 (on observed data)
Refinement	
weighting scheme: $w = 1/(\sigma^2\|F_o\| + (0.01 \times 1.5\|F_o\|)^2)$	no. of refined params: 30
refinement results (on observed reflections): R (%) = 1.83	R_w (%) = 2.36; g.o.f. = 0.89
secondary extinction coefficient: 0.190(8)	type: isotropic, type I, Lorenzian distribution
residual electronic density: [−0.60, +0.81] e$^-$/Å^3	

compounds ($0 \le x < 1$) were prepared according to the procedure described by Huang[8] and Le Rolland:[9,10] finely ground powders of Ce_2S_3 (325 mesh, Cerac, 99.9%), La_2S_3 (−200 mesh, Strem Chemicals, 99.9%), and P_2S_5 (Merk, 99.8%) taken in the aimed stoichiometric ratio were placed in evacuated (10^{-3} Torr) quartz tubes, sealed, and slowly heated at 900 °C for 10 days with an intermediary stage of 2 days at 300 °C. The samples were then slowly cooled to room temperature. All compounds were handled in dry glovebox because of their great air sensitivity. From the very thin microcrystalline powder obtained, $CePS_4$ single crystals were then prepared by transport at 950 °C with iodine (40 mg of I_2 for a silica tube length of about 15 cm and an inner diameter of 1 cm and around 500 mg of $CePS_4$) for 10 days. Well-shaped single crystals were then picked up from the sample bulk for crystallographic analyses.

X-ray Structure Determination

$CePS_4$ Structure Study. X-ray powder diffraction diagrams were recorded on a CPS 120 INEL X-ray powder diffractometer equipped with a monochromatized radiation Cu K-L_2 and a position-sensitive detector calibrated with $Na_2Ca_3Al_{12}F_{14}$ as standard.[11] The powder was sieved at 20 μm and introduced in a Lindemann capillary ($\phi = 0.1$ mm). From the reported tetragonal cell constants, all the diagram reflections were assigned (hkl) indices, indicating a good purity of the sample at the X-ray diffraction detection threshold. Accurate cell parameters ($a = b = 10.9228(3)$ Å, $c = 19.3998(6)$ Å) were extracted from a full pattern matching refinement (FULLPROF[12]) ($R_p = 3.65\%$, $R_{wp} = 4.79\%$, $R_{exp} = 3.88\%$ and $\chi^2 = 1.52$). These parameters agree well with the previously published ones.[8−10]

A $0.10 \times 0.10 \times 0.15$ mm^3 single crystal of $CePS_4$ was selected and mounted on a CAD4 X-ray diffractometer for room-temperature data collection. The single-crystal data collection conditions are reported in Table 1. The structure was solved using the atomic positions of the well-known $LnPS_4$ structural type[13−16] with the JANA98[17] structure determination package. Conventional atomic and anomalous scattering factors were taken from the usual sources. The diffraction data analysis confirmed the previously reported Laue symmetry and space group ($I41/acd$). Semiempirical ψ scan-based absorption corrections were made, and after averaging (547 independent reflections, $R_{int} = 3.19\%$), the refinement cycles led to $R_F = 1.83\%$, $R_w = 2.36\%$, and a goodness of fit of 0.89 (30 variables). The final difference electron density showed features no higher than 0.81 e$^-$/Å^3 and no lower than −0.60 e$^-$/Å^3. The atomic and equivalent isotropic displacement parameters are gathered in Table 2.

Table 2. Fractional Atomic Coordinates and Equivalent Isotropic Atomic Displacement Parameters of $CePS_4$

atom	x	y	z	U_{eq} (Å^2)
Ce(1)	1/2	3/4	5/8	0.0153(3)
Ce(2)	1/2	3/4	3/8	0.0144(3)
P	3/4	0.7128(1)	1/2	0.0141(5)
S(1)	0.7483(1)	0.8194(1)	0.41396(5)	0.0192(4)
S(2)	0.59348(8)	0.61158(9)	0.50198(6)	0.0165(4)

$La_{1-x}Ce_xPS_4$ ($0 \le x < 1$) Compounds Structural Study. For each $La_{1-x}Ce_xPS_4$ compound ($0 \le x \le 1$), the X-ray powder diffraction pattern was found to present a single phase, demonstrating the occurrence of a random La/Ce distribution. The cell parameters were obtained from a full pattern matching refinement.[12] Figures 1a and 1b show the a and c parameter variation versus x. The linear decrease of the cell parameters from $LaPS_4$ to $CePS_4$ is in agreement with the lanthanide contraction law.

Optical Measurements. The room-temperature UV/VIS/NIR diffuse reflectance spectra were recorded on finely ground samples with a Perkin-Elmer Lambda II spectrometer. This instrument was equipped with a 60 mm diameter integrating sphere and computer controlled using the PECOL software. The reflectance versus wavelength measurements were made in the 250−1100 nm range (i.e., from about 1.1 to 5.0 eV) using $BaSO_4$ powder (Perkin-Elmer standard) as reference (100% reflectance). These diffuse reflectivity spectra may be used to obtain values for the band gap which agree rather well with

(9) Le Rolland, B.; Molinié, P.; Colombet, P. *C.R. Acad. Sci.* **1990**, *310*, 1201.
(10) Le Rolland, B.; McMallian, P.; Molinié, P.; Colombet, P. *Eur. J. Solid State Inorg. Chem.* **1990**, *27*, 715.
(11) Evain, M.; Deniard, P.; Jouanneaux, A.; Brec, R. *J. Appl. Crystallogr.* **1993**, *26*, 563.
(12) Rodriguez-Carjaval, J. *Physica B* **1993**, *55*, 192.
(13) Wibelmann, C.; Thesis, Techn. Universität Clausthal, Germany, 1982.
(14) Wibelmann, C.; Brockner, W.; Eisenmann, B.; Schäfer, H. *Z. Naturforsch* **1984**, *39a*, 190.
(15) Volodina, A. N.; Koubchinova, T. B.; Maximova, S. I.; Mouraviev, E. N.; Niazov, C. A.; Tchibiskova, N. T. *Zh. Neorg. Khim. SSSR* **1987**, *32*, 2899.
(16) Palkina, C. C.; Maximova, S. I.; Tchibiskova, N. T. *Zh. Neorg. Mater. SSSR* **1984**, *20*, 1557.
(17) Petricek, V.; Dusek, M. *JANA'98 Crystallographic Computing System*; Institute of Physics, Academy of Sciences of the Czech Republic; Praha, 1998.

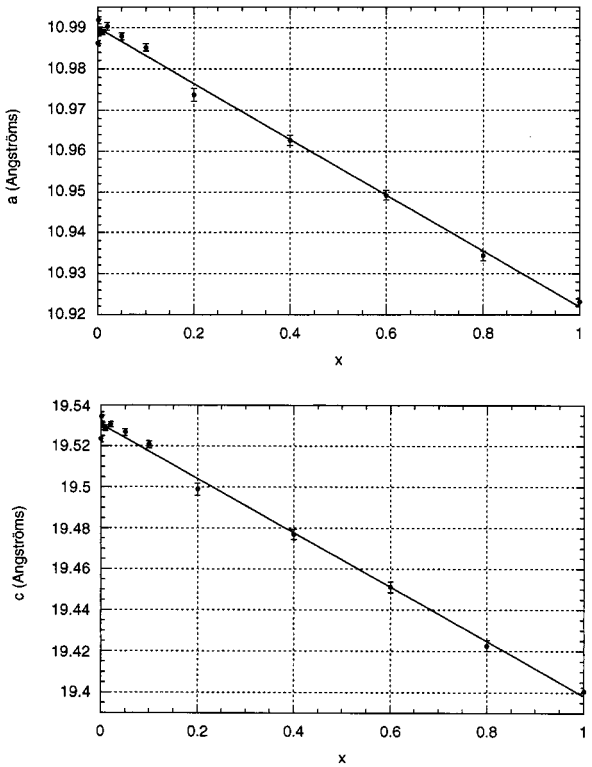

Figure 1. *a* and *c* parameter variations versus *x* in the $La_{1-x}Ce_xPS_4$ series. The linear decrease with *x* is in agreement with the lanthanide contraction law and proves the La/Ce substitution.

those obtained from single crystals. The absorption (α/S) data were calculated from the reflectance using the Kubelka−Munk function:[18−20] $\alpha/S = (1 - R)^2/2R$, where R is the reflectance at a given energy, α is the absorption coefficient, and S is the scattering coefficient. The latter has been shown to be practically energy independent for particle size larger than 5 μm, which is smaller than the particle size of the samples used here. The band gap was determined as the intersection point between the energy axis at the absorption offset and the line extrapolated from the linear portion of the absorption edge in the α/S versus E (eV) plot. Figure 2 gathers the spectra of samples of the $La_{1-x}Ce_xPS_4$ series ($x = 0$, 0.005, 0.01, 0.05, 0.1, 0.4, and 1).

Band Structure Calculations. The self-consistent ab initio band structure calculations were performed on γ-Ce_2S_3 and $CePS_4$ with the tight binding linear muffin-tin orbital method in the atomic-sphere approximation (TB-LMTO-ASA).[21,22] The von Barth−Hedin local exchange correlation potential[23] and the scalar relativistic approximation[24] were used. The space was filled with slightly overlapping Wigner−Seitz (WS) atomic spheres and additional interstitial (or empty) spheres. The optimum radii and positions of these spheres were calculated according to the method described by Jepsen and Andersen.[25] However, as γ-Ce_2S_3 and $CePS_4$ are not close-packed compounds, this calculation step was done with great care. The number of additional empty spheres was first adapted in order to have reasonably big Ce spheres (the calculation was not possible with Ce sphere radii bigger than

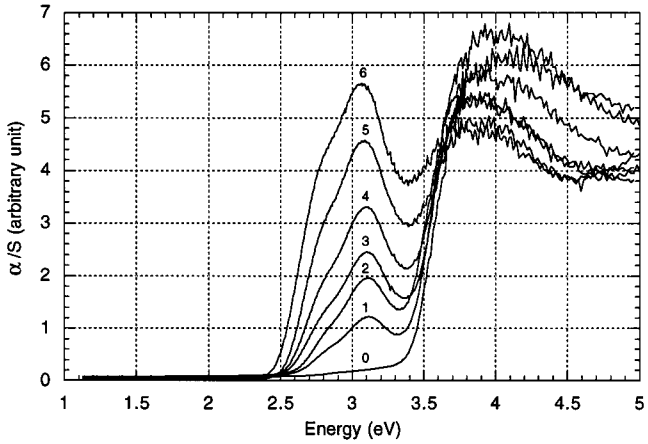

Figure 2. α/S versus energy spectra in the 1.1−5.0 eV range for some $La_{1-x}Ce_xPS_4$ samples: (0) $x = 0$, (1) $x = 0.005$, (2) $x = 0.01$, (3) $x = 0.05$, (4) $x = 0.1$, (5) $x = 0.4$, and (6) $x = 1$).

2.1 Å). The maximum size of the empty spheres was then limited for a more accurate Madelung energy. Finally, a maximum overlap restriction of 16% was applied between the atomic spheres. To take into account the lacunar occupancy of the Ce sites in γ-Ce_2S_3 (in fact $Ce_{8/3}\square_{1/3}S_4$), the calculations were performed in the lower symmetry $I4$ space group (instead of $I\bar{4}3d$ for the Th_3P_4 structural type), conducting to a primitive unit cell of composition Ce_5S_8. The atomic parameters used for the calculation are given for γ-Ce_2S_3 and $CePS_4$ for reference.[26,27]

The full LMTO basis set consisted of the 6s, 6p, 5d, and 4f orbitals for Ce spheres, the 3s, 3p, and 3d orbitals for P and S spheres, and the s, p, and d orbitals for empty spheres (ES). For the eigenvalue problem, the following minimal basis set, obtained using the Löwdin downfolding technique,[28] was used: the LMTO of Ce (6s, 5d, and 4f), P (3s and 3p), S (3s and 3p), and ES (1s). The *k*-space integration was performed with the tetrahedron method [29] and the charge self-consistency was reached with 58 and 13 irreducible k-points for γ-Ce_2S_3 and $CePS_4$, respectively.

For $CePS_4$, bonding information was obtained by computing the crystal orbital Hamiltonian population (COHP)[30] which is the weighted Hamiltonian population density of states. As recommended by Boucher et al.,[31] the basis set used for the COHP calculation was the minimal basis set previously mentioned in which all the empty spheres LMTO's have also been downfolded. In addition, the effect of polarization of phosphorus on the electronic cloud was examined with the help of the representation of the electronic density and of the electronic localized function (ELF). This function introduced by Becke and Edgecombe,[32] following the works by Lennard-Jones,[33] reveals the degree of pairing of the electrons. The

(18) Wendlandt, W. W.; Hecht, H. G. *Reflectance Spectroscopy*; Interscience Publishers: New York, 1966.
(19) Kortüm, G. *Reflectance Spectroscopy*; Springer-Verlag: New York, 1969.
(20) Tandon, S. P.; Gupka, J. P. *Phys. Status Solidi* **1970**, 363−367.
(21) Andersen, O. K. *Phys. Rev. B* **1975**, *12*, 3060.
(22) Andersen, O. K.; Jepsen, O. *Phys. Rev. Lett.* **1984**, *53*, 2571.
(23) von Barth, U.; Hedin, L. *J. Phys. C.* **1972**, *5*, 16229.
(24) Koelling, D. D.; Harmon, B. N. *J. Phys. C* **1977**, *10*, 3107.
(25) Jepsen, O.; Andersen, O. K. *Z. Phys. B* **1995**, *97*, 35.

(26) Since γ-Ce_2S_3 is a phase with a disordered cationic distribution, an ordered arrangement has been considered. It consisted of a C_5S_8 ordered phase. Data used for the band structure calculations are as follows, Space group $I4$, atomic sphere radii (Å) and positions: Ce1 (1.86//0; 0; 0), Ce2 (1.86//1/8; 1/4; 5/8), S1 (1.49//0.3231; 0.9269; 0.0519), S2 (1.49//0.1769; 0.9269; 0.6981). Empty sphere radii (Å) and positions: E1 (1.89//0; 1/2; 1/4), E2 (1.22//0; 0; 1/2), E3 (1.22//1/2; 0; 1/4), E4 (1.22; 1/4; 1/8; 7/8).

(27) For the band structure calculations on $CePS_4$, the data were as follows. Atomic sphere radii (Å): Ce1 (2.00), Ce2 (1.97), P (1.19), S1 (1.18), S2 (1.18). Empty sphere radii (Å) and positions: E1 (1.31// 0.0961; 0.3445; 0), E2 (1.27// 0.2118; 0.0382, 1/8), E3 (1.26//1/4; 0.0329; 1/2), E4 (1.26//0.0204; 0.0139; 0.4296), E5 (1.06//0.2055; 0.3954; 0.1697), E6 (0.96//0.1120; 0.0664; 0.3250), E7 (0.77//0.1804; 0.1621; 0.0726), E8 (0.68//0.3389; 0.1127; 0.1458), E9 (0.58//0.1582; 0.0320; 0.2168).

(28) Lambrecht, W. R. L.; Andersen, K. O. *Phys. Rev. B* **1986**, *34*, 2439.
(29) Blöchl, P. E.; Jepsen, O.; Andersen, O. K. *Phys. Rev. B* **1994**, *49*, 16223.
(30) Dronskowski, R.; Blochl, P. E. *J. Phys. Chem.* **1993,** *97*, 8617.
(31) Boucher, F.; Jepsen, O.; Andersen, O. K. In preparation..
(32) Beck, A. D.; Edgecombe, K. E. *J. Chem. Phys.* **1990,** *92*, 5397.
(33) Lennard-Jones, J. E. *J. Chem. Phys.* **1952**, *20*, 1024.

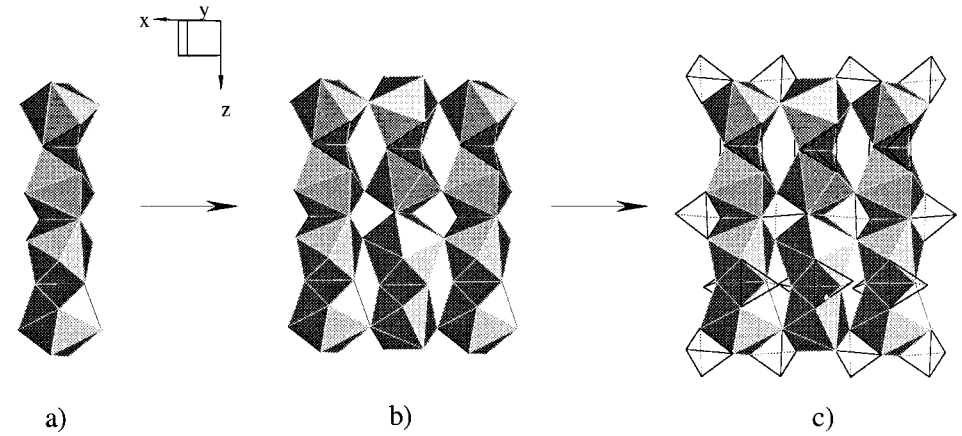

Figure 3. $CePS_4$ structure can be considered as made up from $[CeS_8]$ edge sharing chains (left) sharing corners with neighboring chains along *a* and *b* (middle). Phosphorus cations lie inside $[S_4]$ tetrahedra sharing edges with four adjacent $[CeS_8]$ polyhedra (right).

Table 3. Main Bond Distances (Å) and Angles (deg) in $CePS_4$

Ce(1) environment		Ce(2) environment	
Ce(1)−S(1)	2.950(1) (×4)	Ce(2)−S(1)	2.916(1) (×4)
Ce(1)−S(2)	3.004(1) (×4)	Ce(2)−S(2)	3.065(1) (×4)
P environment			
P−S(1)	2.035(1) (×2)	S(1)−P−S(1)	110.20(8)
P−S(2)	2.036(1) (×2)	S(1)−P−S(2)	108.57(5) (×2)
		S(1)−P−S(2)	107.62(5) (×2)
		S(2)−P−S(2)	114.25(8)

ELF is normalized and found between 0 and 1. If paired electrons with antiparallel spins are localized at an *r* point in the direct space, the ELF at *r* tends to 1. This can thus be seen as corresponding to paired electrons of a covalent bond, or of valence lone pairs. In a homogeneous gas, ELF = 0.5.

Results and Discussions

Structural Aspects. No particular discussion is to be made of the $CePS_4$ structure since the xenotime structural type has been previously reported for other lanthanide phases.[13−16] In this one case, the structural characteristics are those expected (see Table 3), in agreement with the ionic radii and the charge balance: $Ce^{III}P^{V}(S^{-II})_4$. The structure can be considered as constructed from $[CeS_8]$ bicapped prisms and of $[PS_4]$ tetrahedra. Through edge sharing, the $[CeS_8]$ groups constitute, along *c*, infinite chains (Figure 3a). These chains, in turn, share corners with neighboring chains along *a* and *b* to constitute a three-dimensional array (Figure 3b). Phosphorus cations lie inside $[S_4]$ tetrahedron sites resulting from the assembly of two infinite chains (Figure 3c). It results that one $[PS_4]$ tetrahedron shares its edges with those of four $[CeS_8]$ polyhedra of two adjacent chains. The feature relevant to this study (see below) lies in the sulfur atoms being linked to 2 Ce and 1 P.

Optical Properties. To get some insight on the origin of the bright yellow color exhibited by $CePS_4$, our investigations began by measuring the optical properties of this compound through diffuse reflectance experiments. The obtained α/S vs energy spectrum of $CePS_4$ (Figure 2, sample 6**)** shows a steep and well-defined absorption threshold around 2.5 eV, followed by a second one around 3.4 eV. The first steep absorption threshold indicates a good purity of the material, confirming the powder X-ray diffraction data analysis (see above). From the Kubelka−Munk treatment, we can conclude

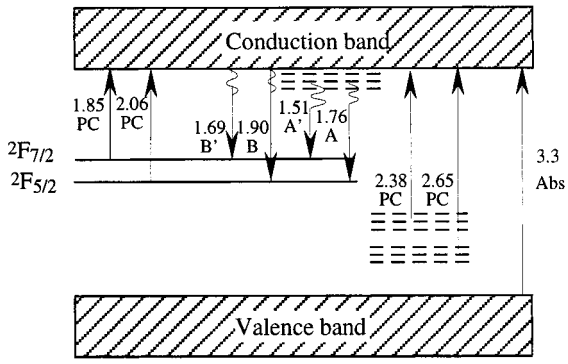

Figure 4. Proposed band scheme for γ-Ce_2S_3 at 77 K (energy in eV) from transitions observed through photoconductivity (PC), absorption (Abs), and fluorescence (A and B) experiments.[3]

the insulating nature of $CePS_4$ with a large energy gap of 2.48 eV. Such a value corresponds to an optical absorption in the blue, resulting in a yellow pigmentation of the material. The second absorption is located in the UV region and, indeed, does not contribute to the chromatic properties of $CePS_4$. Notice the occurrence of a characteristic shoulder in the first threshold, a shoulder originating in the $2F^{5/2}$ and $2F^{7/2}$ spectroscopic terms associated to the $4f^1$ electronic configuration of Ce^{III}.

The red color of γ-Ce_2S_3 (energy gap of ≈1.89 eV)[3] is due to the symmetry and spin-allowed interband, intrasite transition Ce^{III}-$4f^1 \rightarrow Ce^{III}$-$5d^0$, while the S^{2-}(sp) → Ce(5d) indirect and direct charge transfers were found by optical measurement on a single crystal respectively at 2.75 and 3.3 eV in the UV domain.[34] Figure 4 highlights the main band features and electronic transition of γ-Ce_2S_3. With the same cerium sulfur surrounding, a similar mechanism must be involved in $CePS_4$. To confirm this hypothesis, the evolution of the absorption threshold when going from $LaPS_4$ to $CePS_4$, i.e., by substituting the Ce^{III} f^1 optically active species to La^{III} ($4f^0$, $5d^0$) in the colorless $LaPS_4$ matrix, has been studied. The results of this study are shown in Figure 2 for the seven compounds corresponding to $x = 0$, 0.005, 0.01, 0.05, 0.1, 0.4, and 1. For $LaPS_4$

(34) Witz, C.; Huguenin, D.; Lafait, J.; Dupont, S.; Theye, M. L. *J. Appl. Phys.* **1996**, *79* (3), 2038.

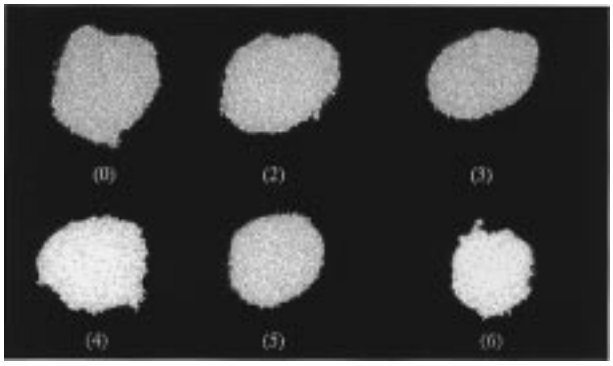

Figure 5. Colors presented by some $La_{1-x}Ce_xPS_4$ solid solutions: (0) $LaPS_4$ ($x = 0$), (2) $x = 0.005$, (3) $x = 0.01$, (4) $x = 0.05$, (5) $x = 0.4$, and (6) $CePS_4$ ($x = 1$).

itself, the energy threshold value is found at 3.41 eV, in good agreement with a colorless material: this absorption corresponds to the valence band (vb) → conduction band (cb) electronic transition. For values of x between 0.005 and 0.1 (curves 1, 2, 3, and 4 in Figure 2), an intense and well-defined absorption peak appears around 3.1 eV that can only be attributed to the introduction of the $4f^1$ levels of Ce^{III} and to the $4f^1 \rightarrow 5d^0$ transition. The positions in energy of these absorption maxima remain quite constant for the low cerium concentrations. For $x = 0.4$, a small shift of the absorption peak is recorded with a maximum slightly below 3.10 eV: this may be attributed to a more important contribution of the Ce^{III} $5d^0$ levels to the transition. Incidentally, this demonstrates that the 5d levels of La and Ce are not energetically very different, as can also be deduced from the fact that the initial absorption edge of $LaPS_4$ is not substantially shifted by the substitution. At the same time, a more and more important absorption threshold develops at lower energy, its position for $x = 0.4$ being close to that of $CePS_4$. These observations show clearly that the yellow color of $CePS_4$ is due to the important $4f^1 \rightarrow$ cb transition of Ce^{III}, the yellow hue being due mostly to the position of the absorption edge itself. In effect, and as can be seen from the color pictures taken for the $La_xCe_{1-x}PS_4$ series (Figure 5), the samples with $x = 0.005$ and 0.01 (samples 2 and 3) appear white-cream in relation with an absorption beginning at around 2.6 eV and having a maximum at 3.1 eV. As soon as the concentration reaches $x = 0.05$ (sample 4), the absorption edge is found at 2.55 eV due to the widening of the 3.1 eV band. For $x = 0.4$ (sample 5) the visual appearance of the phase is practically that of $CePS_4$ itself. This study thus confirms that the electronic absorption mechanism in γ-Ce_2S_3 and $CePS_4$ is the same, only the bandwidth being substantially modified. It is this modification whose origin is now going to be evidenced.

Band Structure Calculations. If the absorption process involved in the color of cerium sulfides appears as well established, the energy separation between the Ce-f and Ce-d block, responsible of the color variation, remains difficult to predict. However, a qualitative approach, through the concept of inductive effect as proposed by Etourneau et al.[7] can be considered to evaluate the trend to be expected in the energy gap changes. Thus, the inductive effect of phosphorus on

Table 4. Observed and Calculated Transition Energies in γ-Ce_2S_3 and $CePS_4$ (This Work and References 3 and 34)

	γ-Ce_{2S3}		$CePS_4$	
	obsd	calcd	obsd	calcd
$4f^1 \rightarrow$ cb	1.89[3]	1.36	2.48	1.00
vb → cb	2.75 (indirect)[34]	2.94	3.41	3.26
	3.3 (direct)[34]			

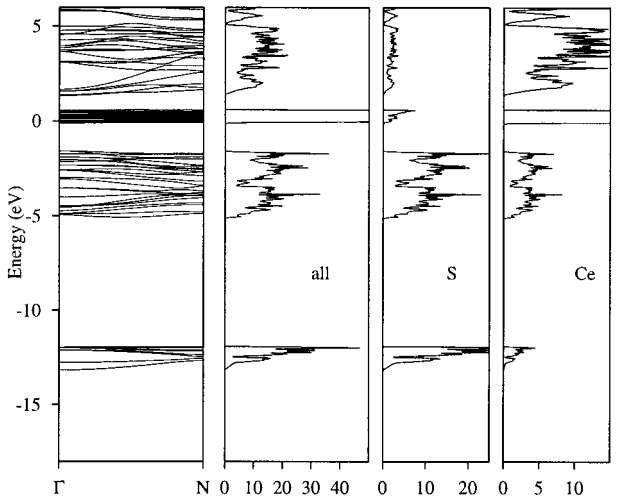

Figure 6. Band structure of γ-Ce_2S_3 along the more dispersed directions and total density of state (DOS) and DOS projected along the different elements.

sulfur must induce a higher ionic character of the Ce−S bond in $CePS_4$ compared with γ-Ce_2S_3, explaining a change in color from red to yellow. Band structure comparisons between these two phases have been done in order to approach more quantitatively the charge redistribution between sulfur and cerium versus the effect of the phosphorus−sulfur bonding.

Concerning γ-Ce_2S_3, even though the band structure has been extensively discussed before,[2,35] we thought it necessary to recalculate it in order to more easily compare its features with those of $CePS_4$. In Figures 6 and 7 are presented the band structure of γ-Ce_2S_3 and $CePS_4$, respectively (along the most dispersed direction), the total density of state (DOS) and the density of state projected along the different elements. The calculations show that, in both cases, the top of the vb is sulfur 3p in character whereas the bottom of the cb is essentially based on the 5d orbitals of cerium. The 4f block (1/14th filled) is situated between the vb and cb blocks (see Table 4). The energy needed to add an electron on a Ce^{III} site is estimated at about 6 eV (Hubbart energy) and this explains why the $4f \rightarrow 5d$ transfer mechanism takes place instead of a vb → $4f^1$ or an intersite $4f^1 + 4f^1 \rightarrow 4f^0 + 4f^2$ one.[36−39] Owing to the highly localized character of the 4f orbitals, and the highly repulsive effect between the intra-cerium 4f electrons, the 4f nondispersed bands cannot lead to any metallic conductivity. Indeed, the calculations agree well with an observed wide-gap semiconducting behavior.

(35) Perrin, M. A.; Wimmer, E. *Phys. Rev. B* **1996,** *54*, 2428.
(36) Hufner, S.; Wertheim ,G. K. *Phys. Rev. B* **1973**, *7*, 5086.
(37) Campagna, M.; Wertheim, G. K.; Baer, Y. *Photoemission in Solids*; Ley, L., Cardona, M., Eds.; Springer-Verlag: Berlin, 1979.
(38) Lang, J. K.; Baer, Y.; Cox, P. A. *Phys. Rev. Lett.* **1979**, *42*, 74.
(39) Lopez-Aguilar, F.; Costa-Quintana, J. *Phys. Stat. Sol. b* **1983**, *118*, 779.

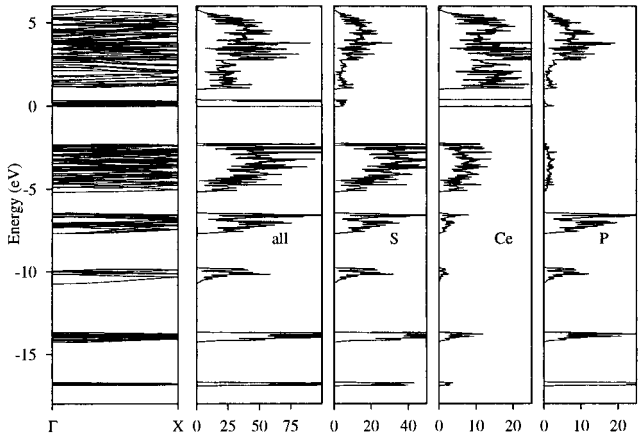

Figure 7. Band structure of $CePS_4$ along the more dispersed directions and total density of state (DOS) and DOS projected along the different elements.

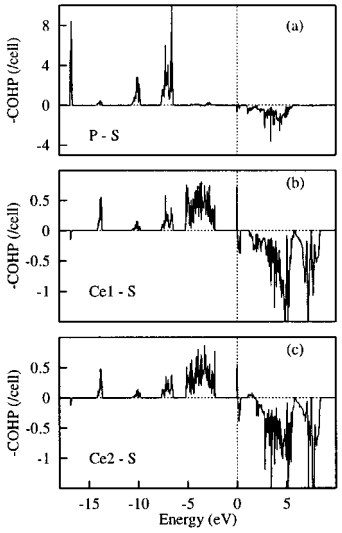

Figure 8. COHP of $CePS_4$: (a) evolution of the COHP versus energy of the P−S mean bonding. (b and c) Ce−S interactions within the anionic bands.

Now the role of the phosphorus cation present in $CePS_4$ on the electronic structure can be addressed, with respect to the relative position of the vb, cb, and 4f levels. Figure 8a gives, for $CePS_4$, the evolution versus energy of the COHP of the P−S mean bonding. It shows that all the bands situated below −5 eV correspond to a bonding character of the P−S interaction. These bands are little dispersed because the $[PS_4]$ groups are isolated from each other by ionic Ce−S bond barriers (see Figure 3), implying that the system could be as well described, as far as the phosphorus groups are concerned, by a molecular orbital scheme rather than by an electronic band one. From this viewpoint, Figure 9 represents a theoretical hybridization scheme of the s and p orbitals of phosphorus and sulfur in the T_d point symmetry. In this scheme are clearly found the four groups of molecular orbitals in which P−S bonding character and positions are in perfect agreement with the (P−S) COHP function of $CePS_4$ (Figure 8a). It is also worth noticing that 8 out of 12 p orbitals of the sulfur atoms of the isolated $[PS_4]$ units have a nonbonding character toward phosphorus but are involved in cerium−sulfur bonding interactions (see below). This character is easily observed in the $CePS_4$ band structure

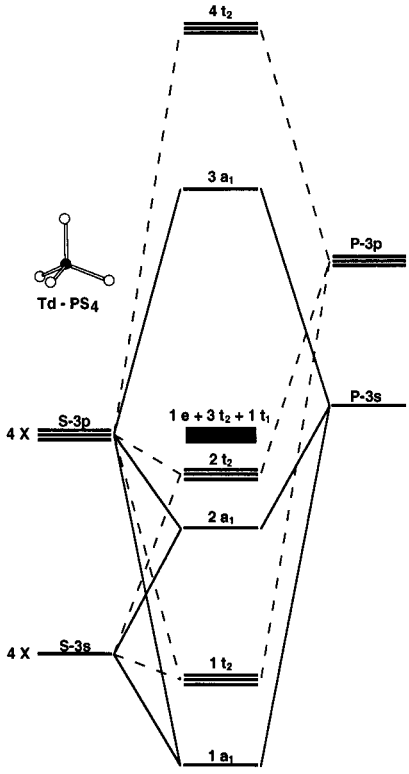

Figure 9. Theoretical hybridization scheme of the s and p orbitals of phosphorus and sulfur in the T_d point symmetry. Nonbonding 1 e, 3 t_2, and 1 t_1 orbitals (see Figure 8) are those engaged in the Ce−S bonds.

since in the [−5, 0] eV energy range the projected phosphorus DOS is practically equal to zero, whereas it is maximum in the projected cerium DOS (Figure 7).

Considering now the Ce − S interactions within the anionic bands (Figures 8b and 8c), one can observe that the Ce atoms give rise to a contribution in the [−20, −1] eV range. Since, with respect to γ-Ce_2S_3, a part of these valence bands is stabilized through the interaction of sulfur atoms with phosphorus (the S-p block ranges from −2.26 to −10.73 eV in $CePS_4$ and from −1.58 to −5.16 eV in γ-Ce_2S_3), it ensues that the electrons engaged in cerium−sulfur bonds are more localized on sulfur in the thiophosphate, showing the inductive effect of phosphorus.

The result of the more ionic Ce−S bond is a decrease of the vb and cb dispersion calculated when going from γ-Ce_2S_3 to $CePS_4$: the bandwidths are of ca. 3.6 and 5.1 eV, respectively, for γ-Ce_2S_3, whereas they are equal to ca. 2.9 and 4.7 eV, respectively, for $CePS_4$ (see Table 4). This results in a change of the vb/cb energy gap (2.94 eV in γ-Ce_2S_3 and 3.26 eV in $CePS_4$), in agreement with the experimental data (single crystals measured indirect gap E_i of about 2.75 eV and direct gap E_g of about 3.3 eV for γ-Ce_2S_3 and powder measured gap of 3.41 eV for $CePS_4$). Concerning the 4f/cb gap, the calculations give an energy of 1.36 and 1.00 eV for γ-Ce_2S_3 and $CePS_4$, respectively, in contradiction to the experimental observations (see optical section), the 4f/cb gap being wider for $CePS_4$ than for γ-Ce_2S_3. It is well-known that the calculations cannot, to date, localize reliably the 4f levels. This means that we can only suggest an origin for the enhancement of the $4f^1 \rightarrow$ cb gap width from the binary to the ternary phase; this suggestion is based on the characteristics found for the vb and cb.

On going from red γ-Ce_2S_3 to yellow $CePS_4$, a 0.59 eV 4f/cb energy difference increase is needed. Even if we consider that the 0.32 eV vb/cb shift is, in one way or another, entirely passed on the 4f → 5d gap, we have to assume that a 4f level energy decrease takes place. This lowering can very well take place owing to the decrease of the cerium 4f screening of the nucleus charge because of the increase of the Ce → S charge transfer from γ-Ce_2S_3 to $CePS_4$, upon the phosphorus inductive action.

To confirm this effect of the P−S bonding, two types of relevant data can be considered: the electronic density and the ELF. In γ-Ce_2S_3 we observe the occurrence of a very good sphericity of the electron clouds around the chalcogen atoms. In $CePS_4$ the same electronic distributions are strongly delocalized toward the phosphorus atoms because of the very strong covalent P−S interaction, whereas a rather regular feature is maintained on the cerium side. A stronger electronic localization is observed on the sulfur atoms in $CePS_4$ with an ELF_{max} of 0.95 compared to γ-Ce_2S_3 with an ELF_{max} of 0.90 assigned to a higher lone pair localization in $CePS_4$ that asserts a higher ionic character of the cerium−sulfur bond in the thiophosphate.

Conclusion

The chromatic properties of $CePS_4$ have been determined and compared to those of the γ-Ce_2S_3. Band structure calculations assert that the origin of color in both materials is a 4f-Ce → 5d-Ce electronic transition. Moreover, the color shift from red for the cerium sulfide to yellow for the thiophosphate has been explained in terms of a negative inductive effect of phosphorus, i.e., a reinforcement of the ionic character of the Ce−S bond under the effect of a main group element. The higher the ionicity of the Ce−S bond, the higher the 4f-Ce → 5d-Ce energy gap. A similar phenomena was at work in Eu^{2+}-doped $BaLiF_3$ and $BaSiF_6$[7,40] where the decrease in energy of the $4f^7 \rightarrow 4f^65d^1$ transition in the former was correlated to an increase of the Eu−F covalency. Nevertheless, even if the inductive effect is a generally understood concept which may be used broadly to better target new synthetic works, band structure calculations are requested to reach a more quantitative approach of the influence on the material properties of the covalency of a bond.

Acknowledgment. The research has been made possible by a grant (CIFRE 260/96) from Rhône-Poulenc Chimie and the "Association Nationale de la Recherche technique".

Supporting Information Available: Crystal structure report consisting of a observed powder pattern, tables of atomic coordinates and anisotropic atomic displacements, and a listing of observed and calculated structure factors (8 pages). Ordering information is given on any current masthead page.

CM980711K

(40) Fouassier, C.; Latourrette, B.; Portier, J.; Hagenmuller, P. *Mater. Res. Bull.* **1976**, *11*, 933.